Mathematical Sciences And Applications E-Notes
Volume 2 No. 1 pp. 1–13 (2014) ©MSAEN

A COMPUTATIONAL MODEL FOR PARTIALLY-PLASTIC STRESS ANALYSIS OF ORTHOTROPIC VARIABLE THICKNESS DISKS SUBJECTED TO EXTERNAL PRESSURE

AHMET N. ERASLAN, YASEMIN KAYA AND BUSRA CIFTCI

(Communicated by Murat TOSUN)

Abstract. A computational model is developed to predict the states of stress and deformation in partially plastic, orthotropic, variable thickness, nonisothermal, stationary annular disks under external pressure. Assuming a state of plane stress and using basic equations of mechanics of a disk, Maxwell relation, Hill's quadratic yield condition, and a Swift type nonlinear hardening law, a single governing differential equation describing the elastic and partially plastic response of an orthotropic, variable thickness, nonisothermal disk is obtained. The solution of this nonlinear second order differential equation subject to free and pressurized boundary conditions is achieved by a shooting method. In this article, we move towards the governing equation by going through basic equations that lead to it and present its solution procedure and some interesting results.

1. Introduction

Because of the importance of basic structures like disks, cylinders, tubes, spherical shells and plates in various branches of engineering, research on the prediction of stress and deformation in these structures is unending [3, 12, 13, 15]. In this regard, the analysis of the mechanical response of rotating or stationary, uniform or variable thickness disks under a variety of loading conditions and comprising different materials have been extensively studied [1, 2, 5, 6, 7, 8, 9, 14, 16, 10, 18]. However, there appear only a few investigations [4, 10] in the literature on disks made of orthotropic material. A thin disk of this type has different material properties in the radial and circumferential directions. The mechanical structure of materials like wood or glass-reinforced plastics is orthotropic.

Date: Received: November 1, 2013 and Accepted: March 14, 2014.
2010 *Mathematics Subject Classification.* 00A69, 70-08.
Key words and phrases. Orthotropic disk, Variable thickness, Elastoplasticity, Hill's quadratic yield criterion, Shooting method.
This article is the written version of author's plenary talk delivered on August 26-29, 2013 at 2nd International Eurasian Conference on Mathematical Sciences and Applications IECMSA-2013 at Sarajevo, Bosnia and Herzegovina.

The objective of the present work is to construct a computational model in order to predict the mechanical response of partially plastic, orthotropic, annular and stationary disks subjected to external pressure. Thickness variability and the existence of a radial temperature gradient are also taken into account. A thin disk, hence a state of plane stress is assumed in the formulation. Using the equation of equilibrium, strain-displacement relations, Hooke's law for orthotropic material, Maxwell relation, Hill's quadratic yield criterion, and a Swift type nonlinear hardening law, a single governing differential equation describing the elastic and partially plastic response of an orthotropic disk is obtained. The numerical solution of this differential equation is obtained by a nonlinear Shooting technique. The resulting IVP system is integrated using Runge-Kutta-Fehlberg fourth-fifth order method to achieve high order accuracy. Newton-Raphson iterations are performed until the boundary conditions are met.

An interesting deformation behavior is observed for disks of small inner radii. Plastic deformation commences at the inner surface and propagates into the disk with increasing pressures. As the pressure further increases, another plastic region appears at the outer surface while the inner plastic region is propagating in the radial direction. Thereafter, the disk consists of three regions: two plastic regions and an elastic region in between. Both plastic regions propagate to cover the elastic region as the pressure increases. Later, the inner elastic region completely disappears and the two plastic regions coincide and hence the disk becomes fully plastic. This behavior is not observed for disks with greater inner radii. The plastic region that commences at the inner surface propagates in the radial direction until it reaches the outer surface so that the disk becomes fully plastic. In this work, both cases are studied and the results are presented in graphical forms.

2. Formulation and Solution

2.1. **Basic Equations.** Dimensionless and normalized variables are used to list the dimensionless forms of the equations for convenience. Thin disk and thus a state of plane stress is presumed. The equation of motion

$$\frac{d}{dr}(hr\sigma_r) - h\sigma_\theta + h\Omega^2 r^2 = 0, \tag{2.1}$$

the compatibility relation

$$\frac{d}{dr}(r\epsilon_\theta) - \epsilon_r = 0, \tag{2.2}$$

and the Maxwell relations for an orthotropic disk

$$\frac{\upsilon_{\theta r}}{E_\theta} = \frac{\upsilon_{r\theta}}{E_r}, \tag{2.3}$$

form the basis [3, 12, 13, 15]. In these equations r is the dimensionless radial coordinate ($r = 1$ at the edge), $h = h(r)$ the dimensionless disk thickness ($h = 1$ at the center), σ_r and σ_θ the dimensionless stress components ($\sigma = 1$ at the yield limit), Ω the dimensionless rotation speed, ϵ_r and ϵ_θ the normalized total strain components, $\upsilon_{r\theta}$ and $\upsilon_{\theta r}$ the Poisson's ratio in $r-$ and $\theta-$ directions, and E_r and E_θ the modulus of elasticity in $r-$ and $\theta-$ directions. A two-parametric parabolic type thickness profile of the form

$$h = 1 - nr^k,$$

with n and k being the parameters, is used in this work to describe the variation of disk thickness along the radial direction.

Introducing the ratio

$$R_1 = \frac{E_r}{E_\theta}, \tag{2.4}$$

the Maxwell relation becomes

$$\upsilon_{r\theta} = R_1 \upsilon_{\theta r}. \tag{2.5}$$

The ratio R_1 is called as the elastic orthotropy parameter. Total strains ϵ_r and ϵ_θ are calculated by superposition of elastic, ϵ_j^e, plastic, ϵ_j^p, and thermal parts, ϵ_j^T, as [15]

$$\epsilon_j = \epsilon_j^e + \epsilon_j^p + \epsilon_j^T. \tag{2.6}$$

Elastic strains are obtained by a combination of the generalized Hooke's Law and the Maxwell relations as

$$\begin{aligned} \epsilon_r^e &= \sigma_r - \nu\sigma_\theta, \\ \epsilon_\theta^e &= R_1\sigma_\theta - \nu\sigma_r, \end{aligned} \tag{2.7}$$

where $\nu = \upsilon_{r\theta}$. The thermal strain is given by

$$\epsilon_j^T = \alpha\Delta T, \tag{2.8}$$

where α is the normalized coefficient of thermal expansion and $\Delta T = \Delta T(r)$ the temperature gradient in the radial direction. The total strain-displacement relations are also important and given by

$$\epsilon_r = \frac{du}{dr}\ , \quad \epsilon_\theta = \frac{u}{r}, \tag{2.9}$$

where u represents the dimensionless radial displacement. The one $u(r) = r\epsilon_\theta$ is generally used to determine the radial displacement.

On the other hand, Hill's quadratic yield condition for an orthotropic disk is given by [11]

$$\sigma_Y = \sqrt{\sigma_r^2 - \frac{2R_2}{1+R_2}\sigma_r\sigma_\theta + \sigma_\theta^2}, \tag{2.10}$$

in which σ_Y is the yield stress and R_2 is another parameter called as the plastic orthotropy parameter. Note that when $R_2 = 1$ Hill's criterion reduces to well-known von Mises criterion. Note also that disk undergoes plastic deformation when $\sigma_Y > 1$. The plastic counterparts of total strains are determined using R_2 as [11]

$$\epsilon_r^p = \frac{\epsilon_{EQ}}{\sigma_Y}\left[\sigma_r - \frac{R_2}{1+R_2}\sigma_\theta\right], \tag{2.11}$$

$$\epsilon_\theta^p = \frac{\epsilon_{EQ}}{\sigma_Y}\left[\sigma_\theta - \frac{R_2}{1+R_2}\sigma_r\right], \tag{2.12}$$

where ϵ_{EQ} represents the equivalent plastic strain. Using a Swift type generalized hardening law, equivalent plastic strain is related to the yield stress according to [7]

$$\epsilon_{EQ} = \frac{1}{H}(\sigma_Y^m - 1), \tag{2.13}$$

where H and m represent two dimensionless hardening parameters.

2.2. **The Governing Differential Equation.** To derive the governing differential equation, first the total strains are written as

$$\epsilon_r = \sigma_r - \nu\sigma_\theta + \epsilon_r^p + \alpha\Delta T, \tag{2.14}$$

$$\epsilon_\theta = R_1\sigma_\theta - \nu\sigma_r + \epsilon_\theta^p + \alpha\Delta T, \tag{2.15}$$

and then substituted into the compatibility equation. After some algebra the result is

$$\frac{1}{R_1}\frac{d\epsilon_\theta^p}{dr} + \frac{d\sigma_\theta}{dr} = -\frac{\epsilon_r^p - \epsilon_\theta^p}{rR_1} + \frac{(1+\nu)\sigma_r}{rR_1} - \frac{(\nu+R_1)\sigma_\theta}{rR_1} + \frac{\nu}{R_1}\frac{d\sigma_r}{dr} - \frac{\alpha}{R_1}\frac{dT}{dr}. \tag{2.16}$$

This is the general equation that governs both elastic and plastic regions. In the elastic region the plastic strains vanish and this equation reduces to

$$\frac{d\sigma_\theta}{dr} = \frac{(1+\nu)\sigma_r}{rR_1} - \frac{(\nu+R_1)\sigma_\theta}{rR_1} + \frac{\nu}{R_1}\frac{d\sigma_r}{dr} - \frac{\alpha}{R_1}\frac{dT}{dr}. \tag{2.17}$$

2.3. **Numerical Solution Procedure.** A stress function of the form

$$Y(r) = h\, r\, \sigma_r, \tag{2.18}$$

is now introduced. Using this definition and the equation of motion, Eq. (2.1), we then express the stresses and their derivatives in terms of the stress function. These equations are

$$\sigma_r = \frac{Y}{h\, r}, \tag{2.19}$$

$$\sigma_\theta = r^2\Omega^2 + \frac{1}{h}\frac{dY}{dr} \tag{2.20}$$

$$\frac{d\sigma_r}{dr} = -\frac{Y}{h\, r}\left[\frac{1}{r} + \frac{1}{h}\frac{dh}{dr}\right] + \frac{1}{h\, r}\frac{dY}{dr}, \tag{2.21}$$

and

$$\frac{d\sigma_\theta}{dr} = 2r\Omega^2 - \frac{1}{h^2}\frac{dh}{dr}\frac{dY}{dr} + \frac{1}{h}\frac{d^2Y}{dr^2} \tag{2.22}$$

Note that, only the derivative of σ_θ contains the second order derivative of Y and in view of Eq. (2.12) the derivative of ϵ_θ^p contains the derivative of σ_θ. Hence, the coefficient of $d\sigma_\theta/dr$ in the governing equation, Eq. (2.16), should be collected by some algebra. Toward this aim, we first determine the derivative of σ_Y. This derivative can be put into the form

$$\frac{d\sigma_Y}{dr} = N_1\frac{d\sigma_r}{dr} + N_2\frac{d\sigma_\theta}{dr}, \tag{2.23}$$

in which

$$N_1 = \frac{(1+R_2)\,\sigma_r - R_2\sigma_\theta}{(1+R_2)\sigma_Y}\ \text{, and}\quad N_2 = \frac{\sigma_\theta + R_2(\sigma_\theta - \sigma_r)}{(1+R_2)\sigma_Y}. \tag{2.24}$$

The derivative of ϵ_θ^p is then determined as

$$\frac{d\epsilon_\theta^p}{d\overline{r}} = \left[\frac{N_1N_4N_5 - N_3R_2\sigma_Y}{H(1+R_2)\sigma_Y^2}\right]\frac{d\sigma_r}{dr} + \left[\frac{N_2N_4N_5 + N_3(1+R_2)\sigma_Y}{H(1+R_2)\sigma_Y^2}\right]\frac{d\sigma_\theta}{dr}. \tag{2.25}$$

where

$$\begin{aligned} N_3 &= \sigma_Y^m - 1 \\ N_4 &= N_3 - m\sigma_Y^m \\ N_5 &= R_2\sigma_r - (1+R_2)\sigma_\theta \end{aligned} \tag{2.26}$$

Hence, after collecting of the coefficient of $d\sigma_\theta/dr$, the governing differential equation, Eq.(2.16), simplifies to

$$N_6\frac{d\sigma_\theta}{dr} = -\frac{\epsilon_r^p - \epsilon_\theta^p}{rR_1} + \frac{(1+\nu)\sigma_r}{rR_1} - \frac{(\nu+R_1)\sigma_\theta}{rR_1} + N_7\frac{d\sigma_r}{dr} - \frac{\alpha}{R_1}\frac{dT}{dr}, \tag{2.27}$$

where

$$N_6 = 1 + \frac{N_2N_4N_5 + N_3(1+R_2)\sigma_Y}{R_1H(1+R_2)\sigma_Y^2}, \tag{2.28}$$

and

$$N_7 = \frac{\nu}{R_1} - \frac{N_1N_4N_5 - N_3R_2\sigma_Y}{R_1H(1+R_2)\sigma_Y^2}, \tag{2.29}$$

Note that in the elastic counterpart of this equation $N_6 = 1$, $\epsilon_r^p = \epsilon_\theta^p = 0$, and $N_7 = \nu/R_1$. Like the stresses and their derivatives, the plastic strains in Eq. (2.27) can be expressed in terms of Y and dY/dr. If all these expressions are substituted into Eq. (2.27), the governing equation can be put into the form

$$\frac{d^2Y}{dr^2} = F\left(r, Y, \frac{dY}{dr}\right), \tag{2.30}$$

which implies a two point boundary value problem. Analytical solution of Eq. (2.30) is not possible as it is quite nonlinear. However, it's efficient and highly accurate numerical solution can be realized by shooting method. This technique is described next.

If we let $\phi_1 = Y$, and $\phi_2 = dY/dr$ the nonlinear boundary value problem described by Eq. (2.30) is transformed into an initial value problem (IVP) of the form

$$\begin{aligned} \frac{d\phi_1}{dr} &= \phi_2, \\ \frac{d\phi_2}{dr} &= F(r, \phi_1, \phi_2). \end{aligned} \tag{2.31}$$

This IVP problem requires initial conditions for its solution. For an annular disk subjected to external pressure the boundary conditions are $\sigma_r(a) = 0$, and $\sigma_r(1) = -P$, where a is the dimensionless inner radius and P the dimensionless external pressure. Therefrom, we obtain the conditions $\phi_1(a) = Y(a) = 0$ and $\phi_1(1) = Y(1) = -h(1)\,P$. However, the initial condition $\phi_2(a)$ is not known. This condition is determined by shooting method combined with Newton-Raphson iterations. If the unknown condition $\phi_2(a)$ is denoted by X, then the nonlinear equation to be solved by Newton-Raphson method takes the form

$$G(X) = \phi_1(1) + h(1)\,P = 0, \tag{2.32}$$

which is derived by imposing the boundary condition $\phi_1(1) = -h(1)\,P$. The iterations begin with the initial estimate $X^{(0)}$ and at each iteration the IVP is integrated three times with the conditions $\phi_2(a) = X^{(k-1)}$ to compute G_1, with $\phi_2(a) = X^{(k-1)} + \Delta X$ to compute G_2 and finally with $\phi_2(a) = X^{(k-1)} - \Delta X$ to

compute G_3, where ΔX is a small increment like $\Delta X \approx 10^{-3}$. A better approximation to $\phi_2(a)$ is then determined from

$$\phi_2(a) = X^{(k)} = X^{(k-1)} - \frac{G_1}{G'}, \tag{2.33}$$

and by central difference

$$G' = \frac{G_2 - G_3}{2\Delta X}. \tag{2.34}$$

The IVP system is solved in $a < r \leq 1$ by Runge-Kutta-Fehlberg Fourth-Fifth order integration method with tight tolerances to obtain accurate results. In this way, when the iterations converge the boundary condition $\phi_1(1) = -h(1)\,P$ is satisfied to at least 8-significant digits.

3. Results of the Computations

In the following $\nu = \upsilon_{r\theta} = 0.3$. In order to visualize the effects of orthotropy parameters R_1 and R_2, computations are performed for a disk of inner radius $a = 0.3$, thickness parameters $n = 0.4$ and $k = 1.2$ and hardening parameters $m = 1.2$ and $H = 0.25$. Keeping R_2 constant at a value $R_2 = 0.85$, the propagation of elastic-plastic border is computed for two different values of R_1 and plotted in Fig. 1. For the disk of $R_1 = 1.15$, plastic deformation commences at the inner face at the elastic limit $P_E = 0.588700$. The plastic region formed here propagates into the disk as the pressure is increased. When the pressure reaches the value $P_I = 0.949741$, another plastic region forms at the outer surface. Thereafter, the disk is composed of three regions: inner plastic, elastic and outer plastic. As the pressure further increases, both plastic regions move into the disk and replace the elastic region. At the pressure value $P_{FP} = 0.987943$, both plastic regions coincide at a radial position $r = 0.7593$ and, as a result, the disk becomes fully plastic. As seen in Fig. 1 for the disk of $R_1 = 0.85$, these stages take place at the critical values $P_E = 0.632735$, $P_I = 0.907899$ and $P_{FP} = 0.978869$. The differences in the deformation behavior between the disks of $R_1 = 1.15$ and $R_1 = 0.85$ are obvious in Fig. 1. For the same disk, the effect of plastic orthotropy parameter R_2 is investigated by keeping R_1 constant at a value of 0.85. The results of the computations for $R_2 = 0.85$ and $R_2 = 1.15$ are plotted in Fig. 2. The differences in the partially plastic response of the disks and the critical values of the pressure can be followed therein.

Similar computations are carried out for a disk of inner radius $a = 0.5$. The parameters used are the same, i.e. $n = 0.4$, $k = 1.2$, $m = 1.2$ and $H = 0.25$. The effect of elastic orthotropy parameter R_1 on the propagation of the elastic-plastic border radius can be seen in Fig. 3. The plastic orthotropy parameter in this figure is $R_2 = 0.85$. The deformation behavior of this disk is somewhat different in nature than that of $a = 0.3$ as depicted in Figs. 1 and 2. As seen in Fig. 3, the plastic region that commences at the inner surface propagates in the radial direction until it reaches the outer surface so that the disk becomes fully plastic. It is also observed in this figure that as R_1 increases, the elastic limit P_E decreases but the fully plastic limit P_{FP} increases. The effect of R_2 on the propagation of elastic-plastic border radius is shown in Fig. 4 for $R_1 = 0.85$. Both disks yield at the inner surface when $P = P_E = 0.466570$ and the plastic region formed here moves in the radial direction with increasing pressures following different paths.

The one with $R_2 = 0.85$ becomes fully plastic at $P_{FP} = 0.673109$, while the other corresponding to $R_2 = 1.15$ becomes fully plastic at $P_{FP} = 0.700345$. The effect of R_2 appears to be an increase in the fully plastic limit.

Taking $P = 0.96$, the stresses and displacement in a disk of $a = 0.3$, $n = 0.4$, $k = 1.2$, $m = 1.2$, $H = 0.25$ and $R_2 = 0.85$ are computed and plotted in Fig. 5. The solid lines in the figure correspond to $R_1 = 1.15$ and the dashed lines to $R_1 = 0.85$. Both disks consist of three regions: inner plastic, elastic and outer plastic. As shown in Fig. 5, the disk with $R_1 = 1.15$ consists of a plastic region in $0.3 \leq r \leq 0.5814$, an elastic region in $0.5814 \leq r \leq 0.9675$ and another plastic region in $0.9675 \leq r \leq 1.0$. When $R_1 = 0.85$, these regions position at $0.3 \leq r \leq 0.5358$, $0.5358 \leq r \leq 0.8528$ and $0.8528 \leq r \leq 1.0$. Although the stresses are not much affected by the variation of R_1, the effect on the displacement is obvious.

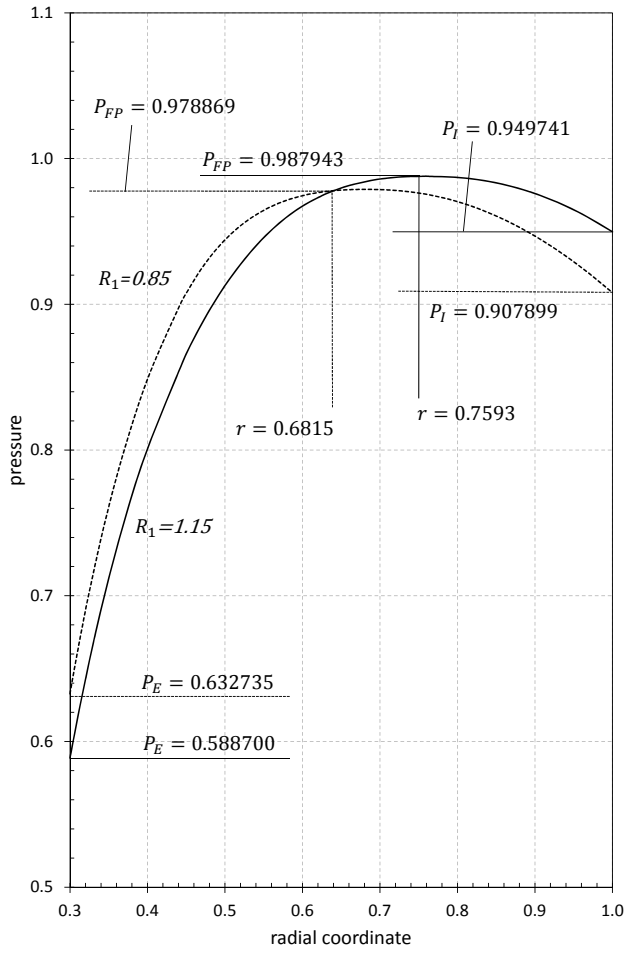

FIGURE 1. Propagation of elastic-plastic border radius for different R_1 values. The parameters used are $R_2 = 0.85$, $n = 0.4$, $k = 1.2$, $m = 1.2$ and $H = 0.25$.

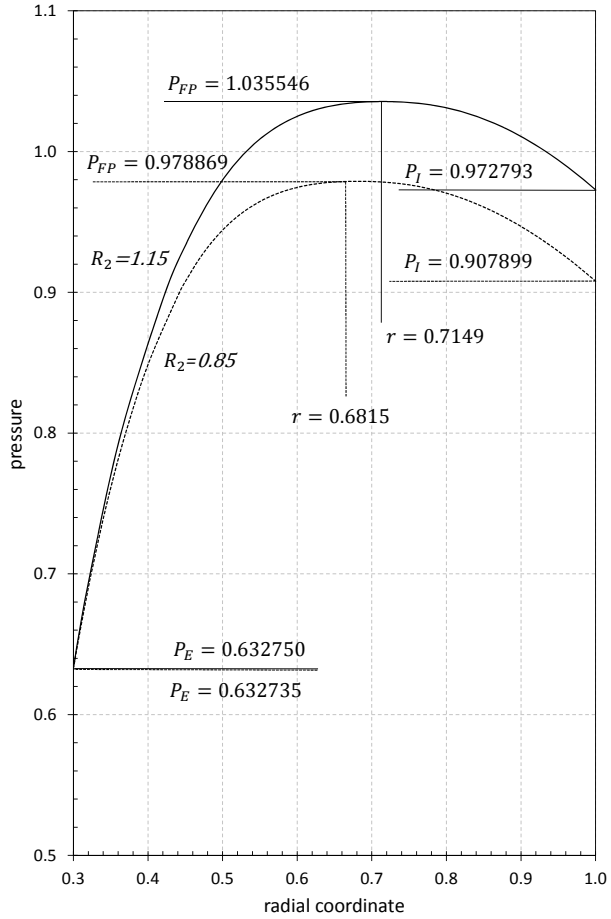

FIGURE 2. Propagation of elastic-plastic border radius for different R_2 values. The parameters used are $R_1 = 0.85$, $n = 0.4$, $k = 1.2$, $m = 1.2$ and $H = 0.25$.

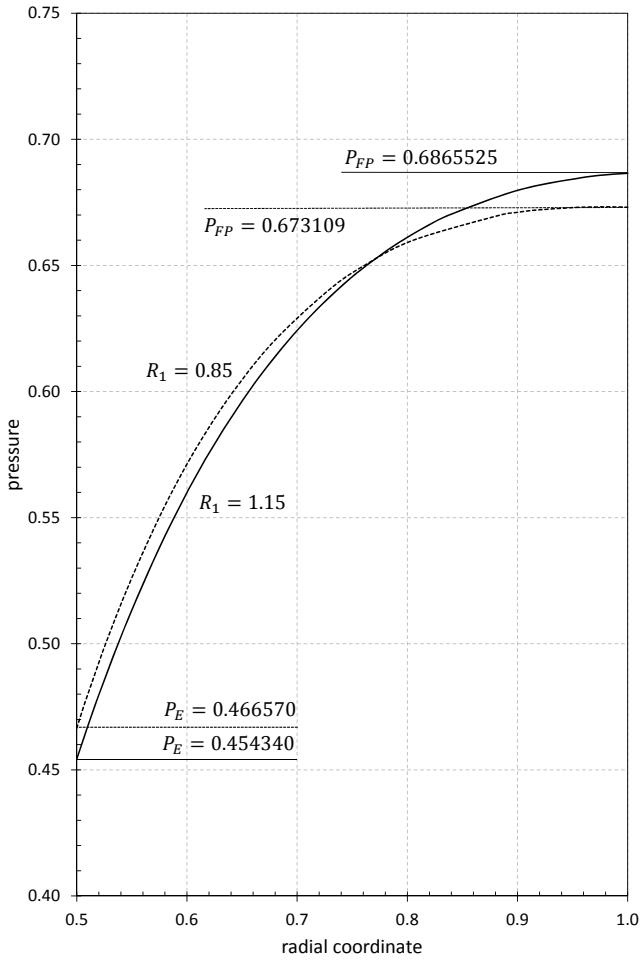

FIGURE 3. Propagation of elastic-plastic border radius for different R_1 values. The parameters used are $R_2 = 0.85$, $n = 0.4$, $k = 1.2$, $m = 1.2$ and $H = 0.25$.

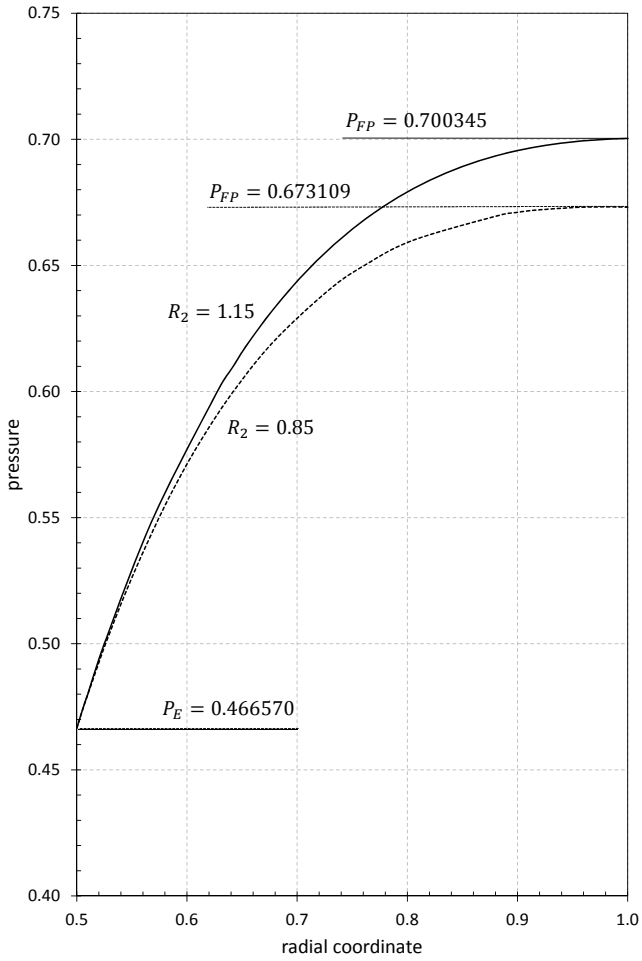

FIGURE 4. Propagation of elastic-plastic border radius for different R_2 values. The parameters used are $R_1 = 0.85$, $n = 0.4$, $k = 1.2$, $m = 1.2$ and $H = 0.25$.

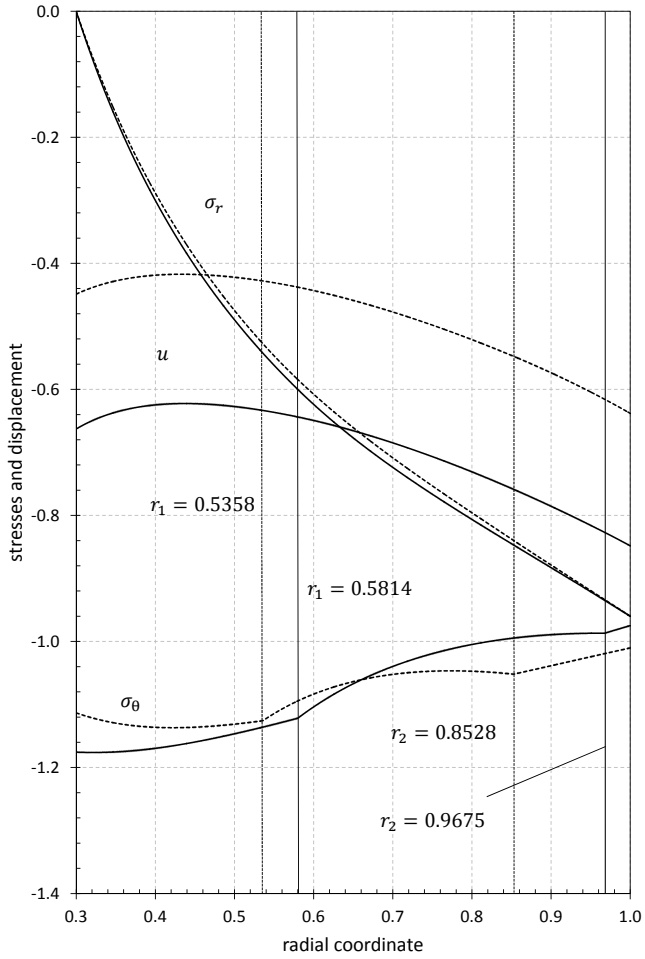

FIGURE 5. Stresses and displacement in an orthotropic disk for different R_1 values. The parameters used are $R_2 = 0.85$, $n = 0.4$, $k = 1.2$, $m = 1.2$ and $H = 0.25$.

References

[1] Argeso, H., Analytical solutions to variable thickness and variable material property rotating disks for a new three-parameter variation function. *Mechanics Based Design of Structures and Machines* 40 (2012), 133-152.

[2] Bayat, M., Sahari, B. B., Saleem, M., Hamouda, A. M. S., and Reddy, J. N., Thermo elastic analysis of functionally graded rotating disks with temperature-dependent material properties: Uniform and variable thickness. *International Journal of Mechanics and Materials in Design* 5 (2009),263-279.

[3] Boresi, A. P., Schmidt, R. J., and Sidebottom, O. M., Advanced mechanics of materials, 5th Ed., Wiley, New York, (1993).

[4] Callıoglu, H., Stress analysis of an orthotropic rotating disc under thermal loading. *Journal of Reinforced Plastics and Composites* 23 (2004),1859-1867.

[5] Eraslan A. N., Stress distributions in elastic-plastic rotating disks with elliptical thickness profiles using Tresca and vonMises criteria. *ZAMM Zeitschrift Fur Angewandte Mathematik Und Mechanik* 85 (2005), 252-266.

[6] Eraslan, A. N., and Akis, T., On the plane strain and plane stress solutions of functionally graded rotating solid shaft and solid disk problems. *Acta Mechanica* 181 (2006), 43-63.

[7] Eraslan, A. N., and Argeso, H., Limit angular velocities of variable thickness rotating disks. *International Journal of Solids and Structures* 39 (2002), 3109-3130.

[8] Eraslan, A. N., and Orcan, Y., Elastic-plastic deformation of a rotating solid disk of exponentially varying thickness. *Mechanics of Materials* 34 (2002), 423-432.

[9] Eraslan, A. N., and Orcan, Y., A parametric analysis of rotating variable thickness elasto-plastic annular disks subjected to pressurized and radially constrained boundary conditions. *Turkish Journal of Engineering and Environmental Sciences* 28 (2004), 381-395.

[10] Gupta, V., and Singh, S. B., Creep analysis in anisotropic composite rotating disc with hyperbolically varying thickness. *Applied Mechanics and Materials* 116 (2012), 4171-4178.

[11] Hill. R., User-friendly theory of orthotropic plasticity in sheet metals. *International Journal of Mechanical Sciences* 35 (1993), 19-25.

[12] Rees, D. W. A., The mechanics of solids and structures. McGraw-Hill, New York, (1990).

[13] Timoshenko, S., and Goodier, J. N., Theory of elasticity, 3rd Ed., McGraw-Hill, New York, (1970).

[14] Tutuncu, N., and Temel, B., An efficient unified method for thermoelastic analysis of functionally graded rotating disks of variable thickness. *Mechanics of Advanced Materials and Structures* 20 (2013), 38-46.

[15] Ugural, A. C., and Fenster, S. K., Advanced strength and applied elasticity, 3rd Ed., Prentice-Hall, London, (1995).

[16] Vullo, V., and Vivio, F., Elastic stress analysis of non-linear variable thickness rotating disks subjected to thermal load and having variable density along the radius. *International Journal of Solids and Structures* 45 (2008), 5337-5355.

[17] You, L. H., Wang, J. X., and Tang, B. P., Deformations and stresses in annular disks made of functionally graded materials subjected to internal and/or external pressure. *Meccanica* 44 (2009), 283-292.

[18] Zenkour, A. M., Stress distribution in rotating composite structures of functionally graded solid disks. *Journal of Materials Processing Technology* 209 (2009), 3511-3517.

Department of Engineering Sciences, Middle East Technical University, 06800, Ankara-TURKEY

E-mail address: aeraslan@metu.edu.tr , kyasemin@metu.edu.tr , bciftci@metu.edu.tr